

The role of rolling friction in granular packing

Yutaka Fukumoto · Hide Sakaguchi · Akira Murakami

Received: 9 August 2011 / Accepted: 2 February 2013
© Springer-Verlag Berlin Heidelberg 2013

Abstract In order to study the effects of the rolling friction of the particles on granular packing, we present a detailed analysis of circular disk assemblies with the rolling friction under macroscopic one-dimensional compression. The rolling friction of the particles produces a resisting moment to the rolling at each contact. A series of 2-D DEM simulations are performed with various values for the rolling friction parameter. We focus on several macroscopic and microstructural properties of granular media and analyze them as a functions of the rolling friction. From these results, we show that the rolling resistance, which results from the rolling friction of the particles, contributes to the inhibition of the rearrangement of the particles and increases the magnitude of the fabric anisotropy under packing. In addition, from both microscopic and macroscopic points of view, we describe that the stress state in a granular packing can vary considerably depending on the rolling resistance.

Keywords Granular packing · Rolling friction · Force transmission · Anisotropy

1 Introduction

The dense packing of granular materials has been the focus of intense research from both numerical and experimental approaches in physics, engineering and other areas

Y. Fukumoto (✉) · A. Murakami
Graduate School of Agriculture, Kyoto University,
Kitashirakawa Oiwake-cho, Sakyo-ku, Kyoto 606-8502, Japan
e-mail: fukumoto.yutaka.84a@st.kyoto-u.ac.jp

H. Sakaguchi
Institute for Research on Earth Evolution, Japan Agency
for Marine-Earth Science and Technology (JAMSTEC),
3173-25 Showa-machi, Yokohama 236-0001, Japan

of research for decades [1–9]. Even today, however, this research topic continues to perplex physicists and engineers. It is especially important to obtain a comprehensive understanding of the properties of the initial packing, which depend on the packing conditions, because these properties are essential to the rheology of granular media.

It should be noted that such particles, consisting of granular materials, are used in many industrial fields and often have irregular shapes. Even if a particle is almost spherical in form, its surface has irregularities or asperities. Due to the features of these particles, rolling at the contacts between the particles can be resisted. Previous experimental and numerical studies have shown that the particle shape strongly affects the quasi-static mechanical behavior of granular materials [7–12]. Therefore, it is important to take account of the effects of the rolling resistance due to particle shape when the packing properties of granular materials are discussed. However, while the importance of the rolling resistance under shear is widely accepted, the effects of the rolling resistance under packing have not been systematically investigated.

In this paper, the packing of compressible granular assemblies with rolling friction is investigated by means of 2-D DEM [13]. Rolling friction means a mechanical property which produces a resisting moment to the rolling at each contact. In this study, we employ circular particles to simplify the investigation process. In order to be able to reproduce the rolling resistance with circular particles, the rolling friction model, which introduces a contact law to the particle–particle contacts, is employed. Then, two-dimensional granular samples are deposited under gravity and compressed in a rectangular box by vertical pressure. They are analyzed at the steady state with various values for the rolling friction parameter.

Firstly, we describe that the influence of the rolling resistance on the volume fraction and the average coordination number. In addition, we investigate the distribution of

contact angles, which give an indication of the fabric anisotropy. Next, we focus on the effects of the rolling resistance on the lateral stress response to a vertical stress applied on the granular system in terms of both macroscopic and microstructural properties. We employ the coefficient of earth pressure at rest as the macroscopic parameter. At the same time, we investigate the angular distribution of normal contact forces from the aspect of the microstructural properties. The relationship between these two properties of stress transmission is also described. Finally, we show the effect of the rolling resistance on the homogeneity of the force distribution in granular media.

The present paper is organized as follows. In Sect. 2, we firstly describe the numerical method, the system characteristics, and the loading parameters. Details of the results of the numerical simulations and discussions are given in Sect. 3. A summary is presented in Sect. 4.

2 Simulation details

2.1 Rolling friction

Several methods have been proposed to model the rolling resistance in DEM [7–12, 14–17]. One method is to directly introduce the geometrical effect using non-spherical particles [7–11] or bonded spherical particles [17]. Another method is to introduce a model for the rolling resistance at the contact point of the spherical particles for the simplicity of its evaluation and lower computational costs [12, 14–16]. The model used in this study is the rolling resistance as a function of the relative rotation and a length parameter is used to represent the contact area as follows.

Figure 1a illustrates two arbitrarily shaped particles i and j are compressed by the normal contact force forming a contact area. We modeled this scenario in two-dimensional DEM with circular particles introducing a contact diameter a on the contact plane to characterize the contact area. In actual

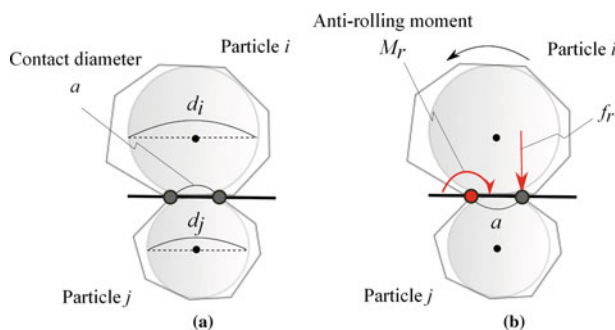


Fig. 1 Rolling friction model. **a** Model of contact area with circular particles for DEM simulations. **b** Anti-rolling moment acting on the particles which rotate

particulate materials, a non-zero contact area may be caused by contact deformation or by particle shape. In this study, however, a is simply given as

$$a = bd, \quad (1)$$

where b is constant and $0 \leq b \leq 1$. Contact diameter a is proportional to particle diameter d regardless of the contact deformation. When particles i and j have different diameters (d_i, d_j), a is determined by the smaller diameter to satisfy the condition in Eq. (1).

Taking the rolling resistance into account, the angular velocity ω for a single particle is calculated as

$$I \frac{\partial \omega}{\partial t} = \sum_1^n (M + M_r), \quad (2)$$

where n is the coordination number of the particle, I is the moment of inertia, M is the rolling moment due to the tangential contact force and M_r is the anti-rolling moment as illustrated in Fig. 1b. The value of M_r is expressed as

$$M_r = -af_r, \quad (3)$$

and f_r is given in consideration of the relative rotation between two particles, θ_r , as follows.

$$f_r = k_n a \theta_r, \quad (4)$$

where k_n is the normal spring constants. Note that Eq. (3) asserts that anti-rolling moment M_r always decreases the magnitude of the angular velocity. In addition, in this model, we give no threshold to M_r in order not to increase the number of input parameters. This assumption is different from other rolling friction models [12, 16] which have a threshold for M_r .

Here, the signs of the relative rotation are obviously different between two particles and the degrees of that are equivalent to each other. Therefore, opposite and equal torques act on these two particles respectively and the angular momentum is conserved.

As described in this subsection, this model requires only one additional parameter b . Thus, it is easy to obtain the corresponding relations between the packing properties and the rolling friction of the particles.

2.2 Packing method

Circular particles are generated in a rectangular box, 200 mm in width and 160 mm in height (see Fig. 2a). In this generation process, the position of each particle is chosen randomly one by one and placed one by one in such a way that there are no overlaps with the particles which have already been placed. The granular system consists of 19,186 particles, which have a particle size distribution of $D_{max}/D_{min} = 3$, $D_{max} = 1.423$ mm, and $D_{min} = 0.474$ mm and a density of

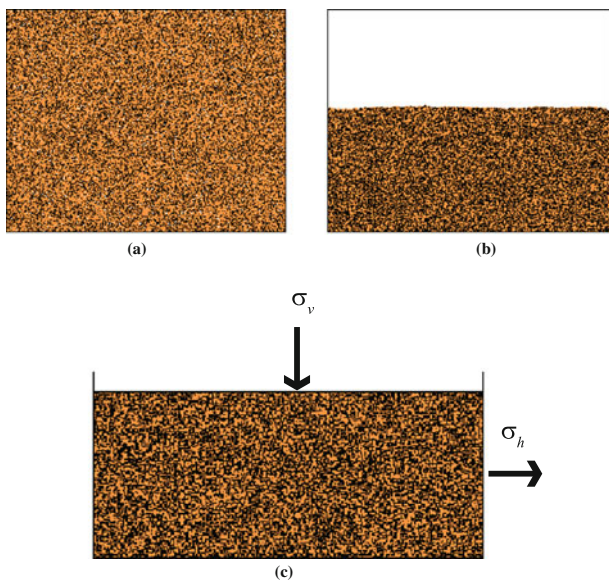


Fig. 2 Packing process for 19,186 granular particles. **a** Particles are randomly placed while avoiding overlap with each other in a rectangular area, 200 mm in width and 160 mm in height. **b** Particles are dropped into the container under the gravity. **c** The compression process is performed by applying vertical pressure to the granular system. σ_v and σ_h indicate the stress acting on the top wall and on the lateral wall, respectively

2400 kg/m². The contact springs are assumed to be linear and $k_n/k_t = 4$ ($k_n = 4.0 \times 10^7$ N/m, $k_t = 1.0 \times 10^7$ N/m), where k_t is the shear spring constants. Rigid walls, whose contact parameters are identical to those of the particles, are assumed for the boundaries. The side walls are fixed and do not move throughout the simulation.

Since the aim of our study is the granular packing in the quasi-static state, we introduce local non-viscous damping [15, 18] in order to achieve the equilibrium state. According to the definition of [15, 18], the damping-force is added to the equation of motion. We constrain the damping to be small enough so as not to have any effect on the results presented in this paper. The non-dimensional value for the damping coefficient is 0.2. In addition, we make the damping force in such a way that it has no effect on the gravitational acceleration of the particles.

In order to study the effect of the rolling friction, different values for rolling friction coefficient b are used. In the preliminary simulations, we observed no particle rotation due to compression for b larger than 0.2. For this reason, we use seven values for b in the range of 0.00–0.15. Moreover, in order to study the combined effect of the inter-particle friction and the rolling friction, three values for μ , namely, 0.08, 0.36 and 0.70, are used. Here, the value for μ of realistic granular materials is up to 1.0. Taking this fact into consideration, we determined the range in the input values for μ . At contacts between the wall and the particles, the inter-particle friction and the rolling friction are set to zero for simplicity.

After specimen generation (see Fig. 2a), the material properties are set for all particles and the simulations are performed by dropping the particles into the bottom of the container under gravity (see Fig. 2b). This sedimentation process is run until the average coordination number and the volume fraction become constant. The simulations are run with a time step of 5.0×10^{-7} s.

The granular samples are then subjected to vertical compression by the top wall for stress control (see Fig. 2c). In this process, the gravity continues to act on the samples. The default position of the top wall is determined so that the particle which has the largest height can just come into contact with the top wall. The constant confining stress acting on the top wall is 100 kN/m, i.e., the value of σ_v/k_n is 0.0025 and the value of $(mg/D)/\sigma_v$ is about 0.00018, where m is a typical particle mass, g is the gravity acceleration and D is a typical particle diameter. These values give the approximate deformation of the grains and the strength of gravity, respectively. In Fig. 2c, σ_v indicates the stress acting on the top wall and σ_h indicates the stress acting on the lateral wall. The compression process is over when the system reaches a steady state. We judge this state by the same criterion as that used in the sedimentation process.

The packing process, described above, is performed with different rolling friction parameters b and inter-particle friction coefficients μ . A total of 21 tests are run. Granular samples are analyzed at the steady state at the completion of the compression.

3 Results and discussions

3.1 Volume fraction and average coordination number

Firstly, we describe the influence of the rolling resistance on volume fraction ν . The value for ν is defined by $\nu = V_p/V$, where V_p is the total volume of the particles and V is the total volume of the packing. The relationship between volume fraction ν and rolling friction coefficient b is reported in Fig. 3. As expected, volume fraction ν decreases with increases in b for all μ cases. This indicates that the rolling resistance inhibits the rearrangement of the particles under packing and that the volume of the voids within the granular samples increase at the steady state.

Next we discuss average coordination number Z , which is the average of the contacts per particle in the contact network, $Z = 2M/N$, where M is the total number of contacts and N is the total number of particles in the contact network. Figure 4 shows the relationship between average coordination number Z and rolling friction coefficient b . From this plot, we can see that the value for Z consistently decreases as b increases for all μ cases. It is thought that the decrease in Z for each μ case

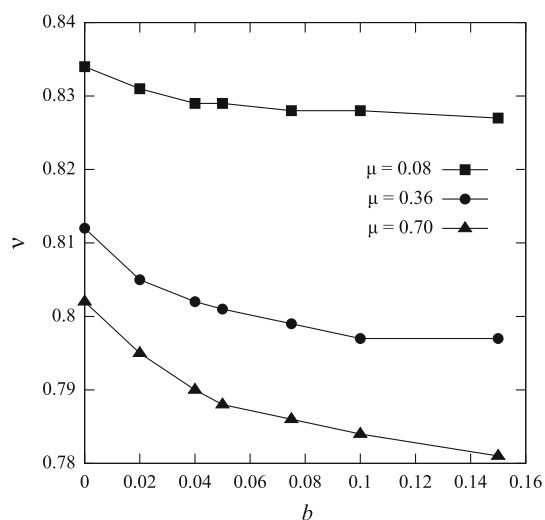


Fig. 3 Volume fraction ν as a function of rolling friction coefficient b for several fixed values for μ

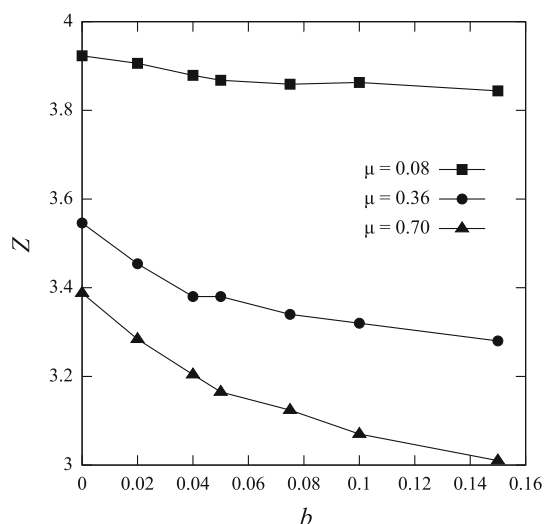


Fig. 4 Average coordination number Z as a function of rolling friction coefficient b for several fixed values for μ

is mainly due to the decrease in volume fraction ν resulting from the rolling resistance.

Additionally, from the analysis in Figs. 3 and 4, for $\mu = 0.08$, as b increases, ν and Z decreases to plateau values of about 0.83 and about 3.9, respectively. This means that the rolling friction has an insignificant influence when the value for μ is small. In contrast, with a large value for μ , the rate of decrease in ν and Z is larger in the other μ cases. That is, as μ increases, the contribution of the rolling friction to the resisting moment becomes large under packing. This trend is in agreement with the recent work involving the investigation of the relative contributions of the inter-particle friction and the rolling friction under shear [19].

On the other hand, Fig. 5 shows the evolution of ν as a function of Z . From this plot, we can see that ν increases with

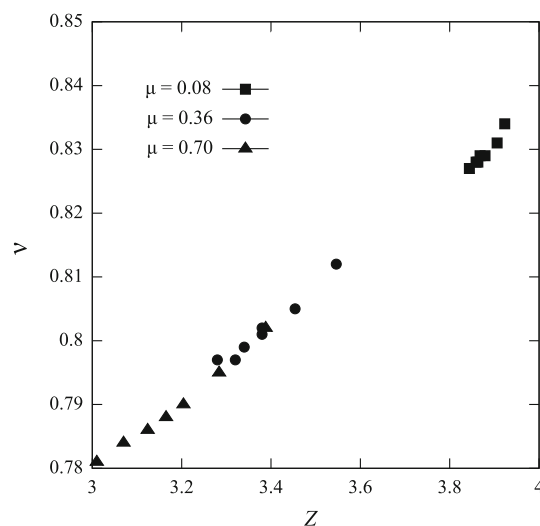


Fig. 5 Volume fraction ν as a function of average coordination number Z

increases in Z regardless of μ or b . In other words, there is a universal relation between ν and Z . This relation implies that the effect of b on ν and Z is almost equivalent to that of μ under packing. Therefore, it can be concluded that the restrain effect on the rearrangement under packing depends on the combination of μ and b .

3.2 Granular fabric

To investigate the granular fabric at the stable state under compression, the distribution of the contact angles, $M(\theta)$, in cases where $\mu = 0.08$ and $b = 0.02$ (\square), $\mu = 0.36$ and $b = 0.05$ (\circ), and $\mu = 0.70$ and $b = 0.15$ (\triangle), is plotted in Fig. 6. In this polar diagram, contact angle $\theta \in [0, 180)$, in degrees, is measured with respect to the horizontal axis in a counter-clockwise direction. For the cases where $\mu = 0.08$ and $b = 0.05$, the fabric is nearly isotropic. In fact, regardless of the b value, this trend is identical if $\mu = 0.08$. This is because the restrain effect on the rearrangement of the particles is very small in such cases. In contrast, for other two cases in Fig. 6, the fabric shows anisotropy. These plots suggest that the magnitude of the fabric anisotropy increases with increases in μ and b . Therefore, the fabric anisotropy also varies depending on the combination of μ and b .

Furthermore, from Fig. 6, we can also see that the directions of the fabric anisotropy correspond to those of the principal stress in this compression system (i.e. the directions of σ_v and σ_h , illustrated as Fig. 2c). In addition, with increasing μ and b , the contacts between the particles decrease along the direction of the minor principal stress. From these results, it can be recognized that the fabric anisotropy under packing, which results from the particle characteristics, arises along the direction of the principal stress.

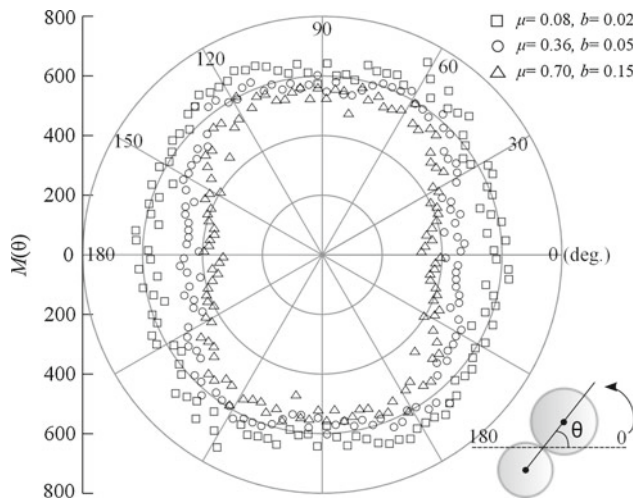


Fig. 6 Polar diagram of the distribution of the contact angles, $M(\theta)$, in the case of $\mu = 0.08$ and $b = 0.02$ (open square), $\mu = 0.36$ and $b = 0.05$ (open circle), and $\mu = 0.70$ and $b = 0.15$ (open triangle). Vertical axis indicates the number of contacts in each contact angle

3.3 Lateral stress response to the vertical stress

Next our investigation is focused on the force transmission in granular media. We employed the coefficient of earth pressure at rest, K , as the expression for the lateral stress response to the vertical stress. This parameter is given in the following:

$$K = \sigma_h / \sigma_v, \tag{5}$$

where σ_h is the lateral stress and σ_v is the vertical stress, which are evaluated by the lateral wall and the top wall, respectively (see Fig. 2c). The value of K indicates a macroscopic property of force transmission in granular media. Figure 7 shows the relationships between K and b . From this figure, we can see that K decreases with increases in b . It is clear that the rolling resistance under packing has an effect on the lateral stress response to the vertical stress. Our data is consistent with the experimental and the numerical studies on the effects of inter-particle bonds on the evolution of horizontal stress under vertical pressure [20]. The rolling resistance and the cementation at the contacts are similar in that both of them prevent the rearrangement of particles under compression.

However, in the case of $\mu=0.08$, K decreases to plateau values of about 0.8 in the same way as for v - b and Z - b . This is because the effect of the rolling friction is small when μ is small, as described in Sect. 3.1. That is, for $\mu = 0.08$, the properties of packing show no significant difference with the value of b . Moreover, the obtained results for $\mu = 0.36$ are about the same as those for $\mu=70$. Therefore, only the case where $\mu = 0.36$ is addressed in the following discussion.

It should be noted that the value for K is usually used in geotechnical engineering to estimate the lateral pressure as a

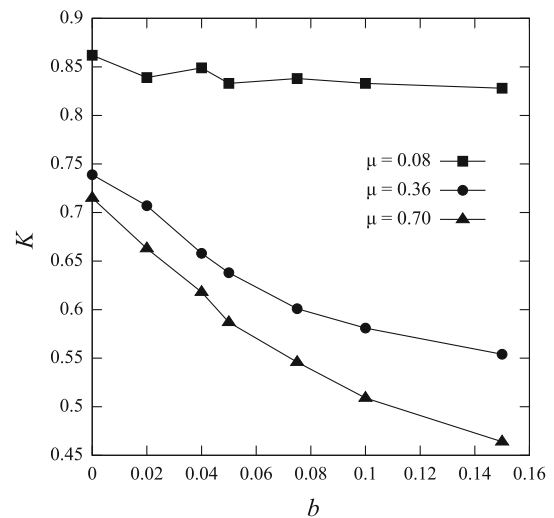


Fig. 7 Coefficient of redirection toward the wall K as a function of rolling friction coefficient b for several fixed values for μ

function of depth under the ground. In addition, the value for K is often described as simply being related to the angle of internal friction of granular materials ϕ [21,22], whereas the value for ϕ is closely related to the rolling resistance [10–12]. Therefore, it is natural to assume that there must be some correlations between K and b . Indeed, our data suggest that the value of K is strongly affected by the rolling resistance of the particles. This observation implies that there is a triadic correlation between K and ϕ and b .

In order to investigate the origin of this macroscopic force transmission, we also study the angular variation in the normal forces from a microscopic point of view, as shown in Fig. 8. Contact angle $\theta \in [0, 180)$, in degrees, is measured in the same manner as in Fig. 6. In this figure, 180 (deg.) is divided into 60 bins of 3 (deg.) each and the average normal force in each bin normalized by the mean normal force, $f_n(\theta) / \langle f_n \rangle$, is plotted against the mean value of that bin for $\mu = 0.36$. Previous studies have shown that this angular distribution is well fitted with just one parameter by Fourier series expressions in sheared granular assemblies [23–26]. According to these studies, our data are fitted by the solid curves drawn in Fig. 8, described by the following equation:

$$\frac{f_n(\theta)}{\langle f_n \rangle} = 1 - A \cos 2\theta, \quad \theta \in [0, 180), \tag{6}$$

where A is the fitting parameter, which corresponds to the amplitude of this “wave”-like distribution. In other words, the value of A is the magnitude of mechanical anisotropy.

From Fig. 8, we can observe that A increases with increases in b . In other words, the rolling resistance broadens the angular distribution of the contact forces. Figure 8 also shows that the contact angle carrying the largest force is 90 (deg.) and that the contact angle carrying the smallest force is 0 (deg.) in all b cases. This observation suggests that the

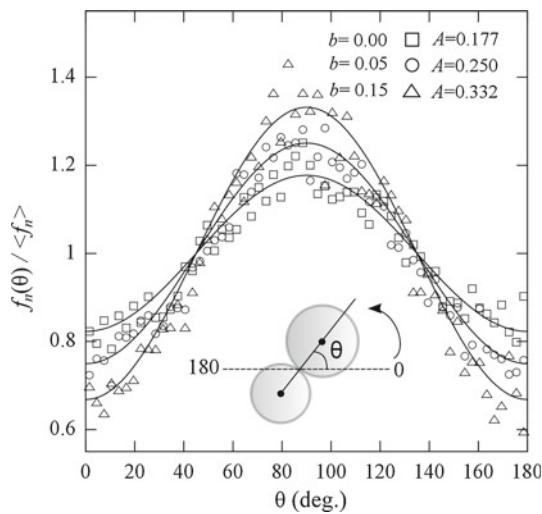


Fig. 8 Angular variation in the normal contact forces in the case of $\mu = 0.36$ for macroscopic one-dimensional compression

directions of these contact angles coincide with those of the principal stress in the macroscopic one-dimensional compression system. From this fact, it can be expected that the amplitude of the mechanical anisotropy contributes strongly to the value of K , which is defined by σ_h / σ_v .

In order to verify the correlation between K and A , we observed the evolution of K as a function of A , as shown in Fig. 9. The solid line is a fitting line described by the following equation:

$$K = -\alpha A + \beta, \tag{7}$$

where both α and β are fitting parameters. The fit of the data to Eq. (7) shown in Fig. 9 is very good; $\alpha = 1.391$, $\beta = 0.997$ and a coefficient of determination R^2 is 0.989. The fitting line indicates that the value of K is about 1.0 when the magnitude of mechanical anisotropy is zero (i.e. $A = 0.0$). Here, it should be noted that we found a clear fitting by Eq. (7) for the granular systems which have relatively anisotropic fabric due to the particle characteristics, as described in Sect. 3.2. In addition, both of the normal contact forces and the tangential contact forces are active in these granular systems.

When this analysis is applied to the granular system, where the fabric is isotropic and the tangential contact forces are not active, the relationship between K and A is derived theoretically from [24] as follows:

$$K = \frac{1 - \frac{1}{2}A}{1 + \frac{1}{2}A}. \tag{8}$$

The curve for Eq. (8) is depicted by the dotted line in Fig. 9. Obviously, we can see that the solid line for Eq. (7) deviates from the dotted line for Eq. (8). It can be expected that this deviation is mainly due to the difference of the analysis conditions, i.e., whether the fabric is isotropic or anisotropic, the

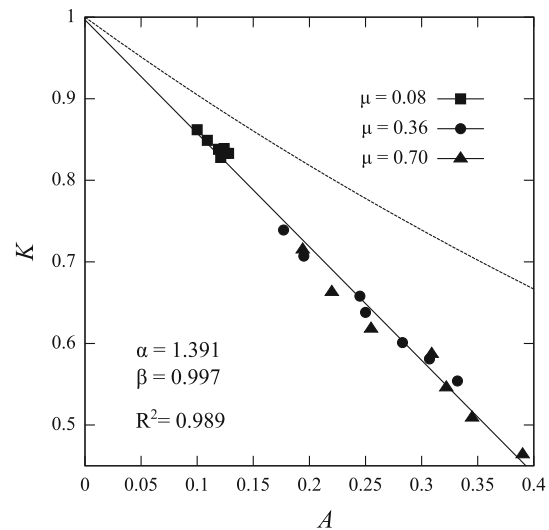


Fig. 9 Correlation between A and K with a solid line: $K = -\alpha A + \beta$ and with a dotted curve: $K = (1-1/2A)/(1+1/2A)$

tangential contact forces are active or inactive and the rolling friction of the particles is present or not.

From these macroscopic and microscopic aspects, it is confirmed that the rolling resistance contributes to the stress redirection in granular assemblies. On the basis of these above findings, we can assume that such a difference in stress states, associated with the rolling resistance, is closely related to the shear strength.

3.4 Force distribution

Finally, in this section, the influences of the rolling resistance on the force distribution is addressed. Figure 10 shows the probability density distribution of normal contact force f_n for $\mu = 0.36$. The normal forces are normalized by the mean normal force $\langle f_n \rangle$. In the inset, a part of function $P(f_n)$ for forces less than $\langle f_n \rangle$ is plotted. Function $P(f_n)$ decays faster for large forces (above the mean normal force) than the exponential and has no clear peak around the mean normal force. Additionally, the force distribution has an upturn at very small forces ($f_n / \langle f_n \rangle < 0.2$). Such trends can also be seen for $\mu = 0.70$. In contrast, the distributions are less sensitive with b for $\mu = 0.08$, where the apparent effectiveness of the rolling resistance cannot be observed.

From the inset in Fig. 10, we can see that the fraction of the particle–particle contacts with very small forces increases with an increasing b , even though the coordination number decreases with an increasing μ . This means that the number of weakly supported particles, which are often termed “rattlers” or “floaters” [27], increases as a result of the enhanced interlocking effect between particles due to the rolling resistance. Moreover, from Fig. 10, it can be observed that as the b increases, the force distribution becomes broad and the

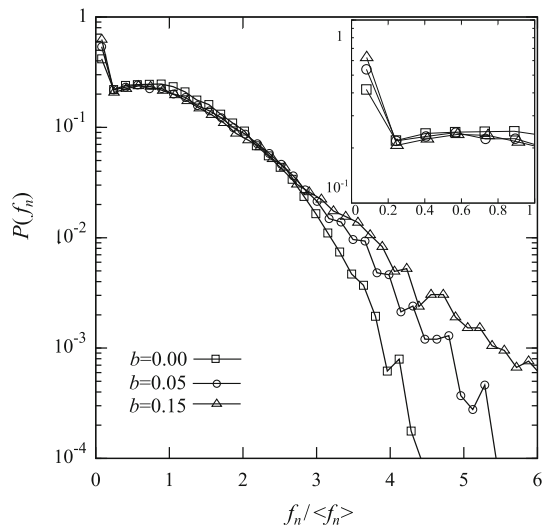


Fig. 10 $P(f_n)$ in the case of $\mu = 0.36$. Normal force f_n is normalized by its mean force $\langle f_n \rangle$

slope of the tail becomes smaller; the fraction of contacts which have large forces also increases. These results show that the stress distribution in a granular packing is less homogeneous in the presence of the rolling friction of the particles. The evolution of inhomogeneous stress distributions, with an increase in b , corresponds to the increase in the magnitude of the mechanical anisotropy, as shown in Fig. 8.

4 Conclusions

We performed a series of 2-D DEM simulations in order to study the effects of the rolling friction of the particles on granular packing. As a result of the analysis, we showed how the rolling resistance, which results from the rolling friction of each particle, plays a role in granular packings, as mentioned below.

Firstly, the rolling resistance was shown to influence the volume fraction and the average coordination number. The obtained data showed that the rolling resistance inhibits the rearrangement of the particles under packing, and its inhibition is almost equivalent to the inhibition effect of the sliding friction. Secondly, we investigate the granular fabric at the stable state and showed that the magnitude of the fabric anisotropy increases along the directions of the principal stresses with increases the rolling resistance. Then, we investigated the lateral stress response to the vertical stress in granular media from the perspective of both macromechanical and micromechanical properties. We found that the stress redirection also varies depending on the value of the rolling friction coefficient, i.e., the rolling resistance reduces the coefficient of earth pressure at rest and broadens the angular distribution of contact forces. In addition, it can be assumed that there are strong correlations between the

rolling resistance and the stress state and the shear strength of granular materials. Finally, we showed that the probability density distribution of normal contact forces, $P(f_n)$, is also affected by the rolling resistance. In other words, the presence of the rolling friction makes the force distribution more inhomogeneous.

In these above findings, the relationship between the stress state and the rolling resistance is particularly important. This is because the stress state is one of the indispensable factors for evaluating the rheology of granular media. Therefore, it is necessary to take into account the rolling resistance when circular or spherical particles are employed in DEM simulations for actually non spherical granular packing.

On the other hand, our findings also imply that the origin of lithostatic pressure, developed in gravitationally deposited granular piles, may be related to the particle shape. Note that lithostatic pressure is a component of confining pressure derived from the weight of the column of rock above a specified level. Further investigation should be done on this point. For example, we plan to analyze the angle of the repose.

It should be noted that many techniques for particle packing have been proposed in DEM simulations [28,29]. Previous research works have revealed that different packing methods have a strong influence on the arrangement of the particles [30,31]. Our observations reported here are based on one of them, namely, that particles are generated randomly and dropped under gravity. Therefore, further studies by means of other packing methods should be also conducted.

References

1. Jaeger, H., Nagel, S., Behringer, R.P.: Granular solids, liquids, and gases. *Rev. Mod. Phys.* **68**, 1259 (1996)
2. Goldenberg, C., Goldhirsch, I.: Effects of friction and disorder on the quasistatic response of granular solids to a localized force. *Phys. Rev. E* **77**, 041303 (2008)
3. Roux, J.N.: Geometric origin of mechanical properties of granular materials. *Phys. Rev. E* **61**(6), 6802 (2000)
4. Makse, H.A., Johnson, D.L., Schwartz, L.M.: Packing of compressible granular materials. *Phys. Rev. Lett.* **84**(18), 4160 (2000)
5. Mueth, D.M., Jaeger, H.M., Nagel, S.R.: Force distribution in a granular medium. *Phys. Rev. E* **57**(3), 3164 (1998)
6. Tighe, B.P., Snoeijer, J.H., Vlugt, T.J.H., van Hecke, M.: The force network ensemble for granular packings. *Soft Matter* **6**, 2908–2917 (2010)
7. Matuttis, H.G., Luding, S., Herrmann, H.J.: Discrete element simulations of dense packings and heaps made of spherical and non-spherical particles. *Powder Technol.* **109**, 278–292 (2000)
8. Rothenberg, L., Bathurst, R.J.: Micromechanical features of granular assemblies with planer elliptical particles. *Géotechnique* **42**(1), 79–95 (1992)
9. Guises, R., Xiang, J., Latham, J.P., Munjiza, A.: Granular packing: numerical simulation and the characterisation of the effect of particle shape. *Granul. Matter* **11**, 281–292 (2009)
10. Lu, M., McDowell, G.R.: The importance of modeling ballast particle shape in the discrete element method. *Granul. Matter* **9**, 69–80 (2007)

11. Matsushima, T., Chang, C.S.: Qualitative evaluation of the effect of irregularly shaped particles in sheared granular assemblies. *Granul. Matter* (2011). doi:[10.1007/s10035-011-0263-6](https://doi.org/10.1007/s10035-011-0263-6)
12. Iwashita, K., Oda, M.: Rolling resistance at contacts in simulation of shear band development by DEM. *Powder Technol.* **109**, 192–205 (2000)
13. Cundall, P.A., Strack, O.D.L.: A discrete numerical model for granular assemblies. *Géotechnique* **29**(1), 47–65 (1979)
14. Sakaguchi, H., Ozaki, E., Igarashi, T.: Plugging of the flow of the granular materials during the discharge from a silo. *Int. J. Mod. Phys.* **7**, 1949–1963 (1993)
15. ITASCA.: PFC2D Theory and Background. Itasca Consulting Group, Inc., Minneapolis (2004)
16. Tordesillas, A., Stuart Walsh, D.C.: Incorporating rolling resistance and contact anisotropy in micromechanical models of granular media. *Powder Technol.* **124**, 106–111 (2002)
17. Utili, S., Nova, R.: DEM analysis of bonded granular geomaterials. *Int. J. Numer. Anal. Meth. Geomech.* **7**, 1997–2031 (2008)
18. Cundall, P. A.: 4 distinct element methods of rock and soil structure. In: Brown, E.T. (ed.) *Analytical and Computational Methods in Engineering Rock Mechanics*, pp. 129–163. Allen&Uwin, London (1987).
19. Estrada, N., Taboada, A., Radjaï, F.: Sear strength and force transmission in granular media with rolling resistance. *Phys. Rev. E* **78**(6), 021301 (2008)
20. Yun, T.S., Evans, T.M.: Evolution of at-rest lateral stress for cemented sands: experimental and numerical investigation. *Granul. Matter* (2011). doi:[10.1007/s10035-011-0279-y](https://doi.org/10.1007/s10035-011-0279-y)
21. Jaky, J.: The coefficient of earth pressure at rest. In *Hungarian (A nyugalmi nyomas tenyezöje)*, *J. Soc. Hung. Eng. Arch. (Magyar Mernok es Épitesz-Egylet Kozlonye)*, pp. 355–358 (1944)
22. Eder, W.: Friction measurements in granular media. *Phys. Rev. E* **69**, 021303 (2004)
23. Bathurst, R.J., Rothenburg, L.: Observation on stress-force fabric relationships in idealized granular materials. *Géotechnique* **39**(4), 601–614 (1989)
24. Radjaï, F., Wolf, D.E., Jean, M., Moreau, J.-J.: Bimodal character of stress transmission in granular packing. *Phys. Rev. Lett.* **80**(1), 61 (1998)
25. Majmudar, T.S., Behringer, R.P.: Contact force measurements and stress-induced anisotropy in granular materials. *Nature* **435**, 1079 (2005)
26. Snoeijer, J.H., Ellenbroek, W.G., Vlugt, T.J.H., van Hecke, M.: Sheared force network: anisotropies, yielding, and geometry. *Phys. Rev. Lett.* **96**, 098001 (2006)
27. O’Sullivan, C.: *Particulate Discrete Element Modelling: A Geomechanics Perspective*. Taylor & Francis, New York (2011)
28. Poschel, T., Schwager, T.: *Computational Granular Dynamics*. Springer, New York (2005)
29. Feng, Y., Han, K., Owen, D.: Filling domains with disks: An advancing front approach. *Int. J. Numer. Meth. Engng.* **56**(5), 699–731 (2003)
30. Geng, J., Longhi, E., Behringer, R.P., Howell, D.W.: Memory in two-dimensional heap experiments. *Phys. Rev. E* **64**, R060301 (2001)
31. Voivret, C., Radjaï, F., Delenne, J.-Y., Youssoufi, M.S.E.I.: Space-filling properties of polydisperse granular media. *Phys. Rev. E* **76**, 021301 (2007)